Carbon 129 (2018) 520–526

Contents lists available at ScienceDirect

Carbon

journal homepage: www.elsevier.com/locate/carbon

Improved efficiency of graphene/Si Schottky junction solar cell based on back contact structure and DUV treatment

Ahmed Suhail*, Genhua Pan, David Jenkins, Kamrul Islam

Wolfson Nanomaterials & Devices Laboratory, School of Computing, Electronics and Mathematics, Faculty of Science & Engineering, Plymouth University, Devon, PL4 8AA, UK

ARTICLE INFO

Article history:
Received 25 September 2017
Received in revised form
12 December 2017
Accepted 15 December 2017
Available online 15 December 2017

Keywords:
Graphene/Si Schottky junction solar cell
s-Shaped kink
Deep UV treatment
Texturing process

ABSTRACT

A graphene/Si Schottky junction solar cell is commonly fabricated by using the top-window structure. However, reported devices have many drawbacks such as a small active area of 0.11 cm^2, s-shape in the *J-V* curves, recombination process of charge carriers at the graphene/textured Si interface, high cost and a complex fabrication process. Here, we report a novel graphene/Si Schottky junction solar cell with a back contact-structure, which has benefits of a simpler fabrication process, lower fabrication cost, and larger active area in comparison with a device fabricated with the previous structure. Additionally, we found that the PMMA residue left on graphene surfaces is the key to eliminate the s-shape in the *J-V* curves. Thus, the deep UV treatment of the CVD graphene is applied within the wet transfer process to effectively remove the PMMA residue, suppress the behavior of s-shaped kink in *J-V* curves and enhance the solar cell efficiency. As a result, the recorded power conversion efficiency of 10% is achieved for graphene/textured Si devices without chemical doping and anti-reflection coating, and this value is improved to 14.1% after applying chemical doping. Doped devices also show great stability and retain 84% of the efficiency after 9 days storage in air.

1. Introduction

The attractive properties of graphene, such as near-zero band-gap, high electrical conductivity, high mobility, flexibility, and high transparency have stimulated a lot of research interest [1]. One of the promising applications for graphene is in a graphene/silicon Schottky junction solar cell. To fabricate this device, there are two structures reported so far [2]. The first structure is with a top-window as shown in Fig. S1a [3]. The maximum efficiency of this device is 12.4% after applying the optimal native oxide of Si substrates, forming gas and chemical doping of graphene [4]. However, reported devices with this structure generally have some serious disadvantages such as, a small active area of about 0.11 cm^2, high cost and a complex fabrication process. Additionally, applying the texturing process to this structure causes serious recombination process of carriers at the graphene/textured Si interface for devices as graphene layers are placed on the textured side of Si substrates [5,6]. Recently, graphene/Si Schottky solar cells based on a top-grid structure (see Fig. S1b) have been reported as having a larger active area, lower cost and an easier fabrication process, in comparison with devices fabricated with the top-window structure [2]. Nevertheless, the performance of prepared devices with a graphene area larger than 0.1 cm^2 is degraded. Moreover, fabricated devices suffer from absorption loss due to the front grid electrode and a distinctive s-shaped kink in the measured *J-V* curves. In several devices based on the top-window structure [3,4,6–11], there was also a distinctive s-shaped kink in the measured *J-V* curves. In fact, the s-shaped kink affects the performance of graphene/Si Schottky solar cells by reducing the fill factor [3,7–14]. It has been reported that there are many reasons for the s-shaped kink effect. For example, it was suggested that the s-shape is due to the limitation of accessible states for the holes in graphene [10,14]. It was also stated that this effect attributes to carrier recombination losses at the graphene/Si interface, and this could be reduced by using GO as a passivation layer for the silicon surface [15]. In several cases, the s-shape could also be eliminated when the graphene doping level is enhanced using chemical doping or electrostatic gating [8–10,14], but after sometime the s-shape would be observed again in the *J-V* curves [16]. In a recent study [17], it has been described that this shape is completely eliminated by

* Corresponding author.
E-mail addresses: ahmed.suhail@plymouth.ac.uk, ahmed.198381@yahoo.com (A. Suhail).

https://doi.org/10.1016/j.carbon.2017.12.053
0008-6223/

reducing the PMMA residue and enhancing p-doping in graphene using a forming gas treatment with a specific mixed ratio (Ar/H_2 (50:50)) at 400 °C. Using this procedure Song et al. [4] found that there was still an s-shape in the *J-V* curves of devices treated with the forming gas at 350 °C for 2 h, and it was stated that this issue could be eliminated by applying the optimal native oxide of Si substrates [4]. It has also been reported [18–20] that the forming gas treatment does not remove the PMMA residue properly. To date, the main reason for the existence and subsequent removal of the s-shape kink in the *J-V* curve is still unclear!

Herein, we demonstrate a graphene/Si Schottky solar cell with a new back-contact structure, which has benefits of larger active area (0.19 cm^2), more effective applying texturing process within the fabrication process to reduce the reflected light from the front of Si substrates, simpler fabrication process and lower fabrication cost in comparison with a device fabricated with the top-window structure. We also introduce a deep UV (DUV) treatment in air for 20 min to effectively remove the PMMA residue and suppress the s-shape in *J-V* curves. Additionally, the DUV treatment is applied between 30 and 60 min to reduce the PMMA residue more and enhance p-doping in graphene, resulting in a further improvement in the solar cell efficiency. The chemical doping is also employed to further improve the solar cell efficiency.

2. Experimental section

2.1. Device fabrication

To texture the front surface of substrates, n-type (100) single c-Si substrates with a resistivity of 2–3 Ωcm^{-1}, 0.19 cm^2 area and thickness of 200 μm were cleaned in a solution $NH_4OH:H_2O_2$: H_2O (1:1:5) for 10 min. Afterwards, substrates were immersed in 25 wt% KOH solution for 2 min to remove the saw damage. Then, optimal solution of KOH/IPA/DI H_2O using process c (see Section 3 in supporting information) was used for texturing the front surface of Si substrates. To prepare solar cell devices, both textured and non-textured silicon substrates were cleaned with an RCA procedure to eliminate the metal ion contaminations. At that moment, Si substrates were immersed in a diluted 2% HF solution for 30 s to remove the oxide layer. Later, passivation process was achieved by exposing both substrates for ambient air for 2 h [4,21,22]. Subsequently, 3.3 × 3.3 mm^2 monolayer CVD-graphene area, which is the recommended area to obtain a high graphene/Si solar cell efficiency [2,4], was directly transferred onto the central area of Si substrates (see Fig. 1b, c and d) using the process in our previous work (see supporting information) [23]. At that time, Cr/Ag layers were formed as cathode on the backside (unpolished side) of substrates as shown in Fig. 1e. For a grid electrode, Cr/Au layers, which provide a low resistance contact to the graphene layer [22,24,25], were created onto the surface of graphene. To obtain p-doped graphene sheets, 65%HNO_3 was applied for 60 s.

2.2. Device characterization

X-ray photoelectron spectroscopy (XPS) (Kratos AXIS Ultra DLD spectrometer, monochromatic Al Kα emission at 1486.6 eV with an operating power of 150 W) was used to examine the amount of PMMA residue on the transferred graphene surface. The photovoltaic characteristics of solar cell devices, which were calibrated by a standard Si solar cell, were measured using a keysight B1500A Semiconductor Analyser and a solar simulator under AM1.5 conditions, with an illumination intensity of 100 mW/cm^2. PVE300 system was used to obtain the external quantum efficiency (EQE) of the solar cells.

3. Results and discussion

To overcome the disadvantages of fabrication process for reported graphene/Si Schottky junction solar cells, the new graphene/Si Schottky junction solar cell with a back-contact structure is prepared as shown in Fig. 1. The DUV treatment for 20 min in our previous work as shown in Fig. 1c was also applied before removing the PMMA layer in order to effectively remove the PMMA layer with less residue [23]. The device structure is shown in Fig. 1f, and it has a number of advantages. In particular, the active area of our device is increased for the same recommended area of graphene sheet [2,4], compared with those of the previous devices (see Figs. S1a, S1b and S1c in supporting information). This means that the number of photons absorbed is higher and leads to an increase in the solar cell efficiency as confirmed by the external quantum efficiency data described later. The second advantage of this structure is that texturing process could effectively be involved within the fabrication process of devices. In this case, the process is only applied to the front surface of Si substrates, and graphene layers are placed on the non-textured side of Si substrates. This would avoid the recombination process of carriers between the graphene and textured surface of Si substrates, which occurred in the reported work [5]. The Schottky junction in this structure is formed at the interface between the graphene and silicon as shown in Fig. 2a. As shown in this figure, carriers are generated throughout the whole Si wafer thickness by the incident light.

Then, generated carriers will be separated by the built-in field at the graphene/Si junction. After that, electrons and holes will move in opposite directions, resulting in the generation of the photocurrent [3,26]. Fig. 2b shows the current density-voltage (*J-V*) characteristics of graphene/n-Si Schottky junction solar cells treated with and without DUV. It can be noticed that there is s-shape in the *J-V* curve (black line) of a device based on the back-contact structure and acetone treatment. The short-circuit current density (J_{SC}), open circuit voltage (V_{OC}), fill factor (*FF*) and power conversion efficiency (*PCE*) of this device were 19.5 mA/cm^2, 0.415 V, 23% and 1.87%, respectively. In contrast, there is a typical *J-V* curve (blue line) of a device based on the back-contact structure and DUV treatment for 20 min. The values of photovoltaic parameters for this device were 32.9 mA/cm^2, 0.41 V, 35% and 4.7%, respectively. It is clear that minimizing the PMMA residue would eliminate the s-shape, resulting in an increase of the *FF* by 55% compared with that of the sample treated with acetone only.

It is also observed that reduction of this residue would also enhance the J_{SC}. This indicates that PMMA residue would act as traps for generated carriers during their transmits at the interfaces through the solar cell device, leading to an increase in the recombination process [23,27]. Recently, it has been confirmed that this residue would also affect the separation process obtained by the built-in field for generated carriers at the junction of graphene/Si [17]. This data also shows that the V_{OC} of the sample is slightly decreased after DUV treatment. This means that graphene becomes less p-doping [23,28]. Hence, this confirms that removing the PMMA residue is the key to eliminate the s-shape in *J-V* curves of graphene/n-Si Schottky junction solar cells. It has also been shown that applying DUV treatment for 20 min is faster, safer and easier to remove the PMMA residue and eliminate the s-shape, compared with that of recent work [17]. To compare the performance of our device, a device with active area of 0.11 cm^2 was prepared using the top-window structure. Fig. 2b compares the *J-V* curves of graphene/n-Si Schottky junction solar cells fabricated with both structures. The J_{SC}, V_{OC}, *FF* and *PCE* of the device fabricated with the top-window structure were 26.7 mA/cm^2, 0.41 V, 31% and 3.4%, respectively. It is obvious that an increase in the active area of our device results in an improvement of the *PCE* by 40%, compared with

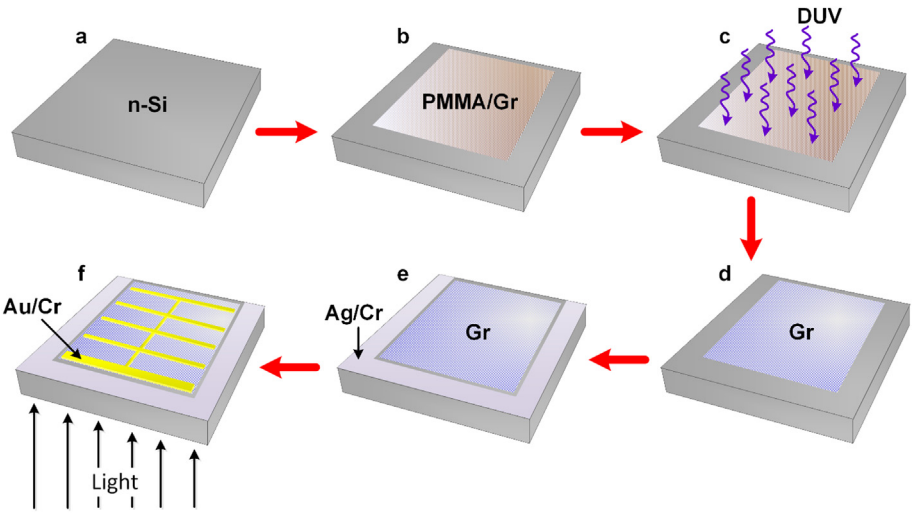

Fig. 1. Fabrication process of graphene/Si Schottky junction solar cells. (a) Si substrate after cleaning process and leaving in air for passivation process for 2 h. (b) Transferring PMMA/graphene (Gr) onto the center of Si substrate. (c) Exposing PMMA/Gr to the DUV of 254 nm at 180 °C. (d) Removing PMMA layer by acetone treatment. (e) Creating Ag/Cr cathode. (f) Forming Au/Cr grid. (A colour version of this figure can be viewed online.)

that of the previous device. Hence, applying the back contact structure within the fabrication process of graphene/Si solar cells is a smart idea to increase the active area of solar cell with using the recommended area of graphene sheets. Fig. 2c shows the external quantum efficiency (EQE) spectra of both devices. As shown in this figure, an EQE of the device fabricated with back-contact structure was about 65% in the wavelength range of 400–950 nm, whereas it was 53% for the device fabricated with top-window structure within the same range. It is clear that the EQE spectrum of our device shows a significant increase in the number of electron-hole pairs generated and collected after increasing the active area of device, compared with that of the device fabricated with top-window structure. In addition, our device shows the highest EQE spectrum in comparison with those for reported pristine graphene/Si Schottky junction solar cells prepared with top-grid and top-window structures [2,25]. Based on the EQE-setup method [29], the calculated values of J_{SC} were 31.6 and 25.8 mA/cm^2 for devices fabricated with back-contact and top-window structures, respectively, which were in agreement with those experimentally obtained from *J-V* curves in Fig. 2b. The effect of DUV treatment for longer periods (between 30 and 65 min) on the performance of this device was also systematically investigated. Average results of measured photovoltaic parameters for each exposed device are shown in Fig. 3.

As observed in Fig. 3a, the V_{OC} and J_{SC} significantly increased to 0.51 V and 33.8 mA/cm^2, respectively after DUV exposure of PMMA/graphene for 60 min. These enhancements improved the *FF* to 39% and *PCE* to 6.7% as shown in Fig. 3b. There were two reasons for this improvement. The PMMA residue was further minimized by applying the DUV for longer time than 20 min as confirmed by X-ray photoelectron spectroscopy (XPS) (see Fig. S5), in comparison with that of graphene layers treated with DUV for 20 min. The second reason results from the p-type doping effect obtained by DUV in graphene when samples were exposed to the DUV for longer than 20 min periods. This doping was investigated using Raman spectroscopy. Raman data shows that there was a significant blue shift in the spectrum of graphene sheet exposed to the DUV for 60 min, compared with that of a sample treated for 20 min as illustrated in Fig. S4. This confirms that applying this treatment for longer than 20 min would enhance p-doping in graphene [17–20,30]. The I_{2D}/I_G peak intensity ratio of exposed graphene for 20 min was around 2, and it was 1.8 for graphene treated for 60 min. It can also be observed that there is no D band in the spectrum of exposed graphene for 60 min. This data indicates that the transferred graphene layer with DUV for 60 min was still a high-quality monolayer [31]. This means that the mechanism of the DUV treatment between 30 and 60 min is to further reduce the PMMA residue and enhance p-doping in graphene, resulting in a further improvement in the solar cell efficiency.

This mechanism is the same of that of the forming gas, but the forming gas would not effectively remove the PMMA residue [18–20], compared with DUV treatment. Furthermore, it has been confirmed that the p-doping obtained by DUV light is more effective than that obtained by forming gas method as the I_{2D}/I_G ratio of graphene will be around 1 after annealing process. In addition, forming gas method has to be carried out in vacuum for few hours [17–20], whereas the DUV treatment was applied in air for 1 h. Hence, applying DUV treatment between 30 and 60 min is more effective, faster, safer and easier to remove the PMMA residue and enhance p-doping in graphene, in comparison with that of forming gas treatment. We have tried to further improve the performance of devices by applying the DUV for longer time. The V_{OC} and J_{SC} slightly increased to 0.52 V and 33.9 mA/cm^2, respectively after treating PMMA/graphene devices for prolonged DUV exposure as shown in Fig. 3a. However, the *FF* and *PCE* observably decreased to 33% and 5.8%, respectively due to the s-shape in *J-V* curve (red line) as shown in Fig. 4. To show that the PMMA residue was the main reason for the s-shape, XPS was also employed. Fig. 5a shows the C 1s core-level spectra of the treated sample for 65 min. It is obvious from this figure that there are five peaks, the black peak represents the overall XPS curve, the red peak (Sp^2) corresponds to graphene, and the other peaks (Sp^3, C–O and C=O) indicate the PMMA residue [17,23,28]. The peaks attributed to the PMMA residue can be clearly observed in Fig. 5a.

This indicates that irradiation of PMMA/graphene sheets for longer time than 60 min resulted in over baking of the PMMA layer, and this caused PMMA residue on the graphene surface after acetone treatment, resulting in the s-shape. Raman data also shows that there is a D band in the spectrum of exposed graphene for 65 min (see Fig. S4). This states that the transferred graphene with DUV for 65 min was not a high-quality monolayer. Hence, it is recommended that the DUV treatment should be applied between 20 and 60 min within the wet transfer process of CVD-graphene in order to remove the PMMA residue and improve the performance

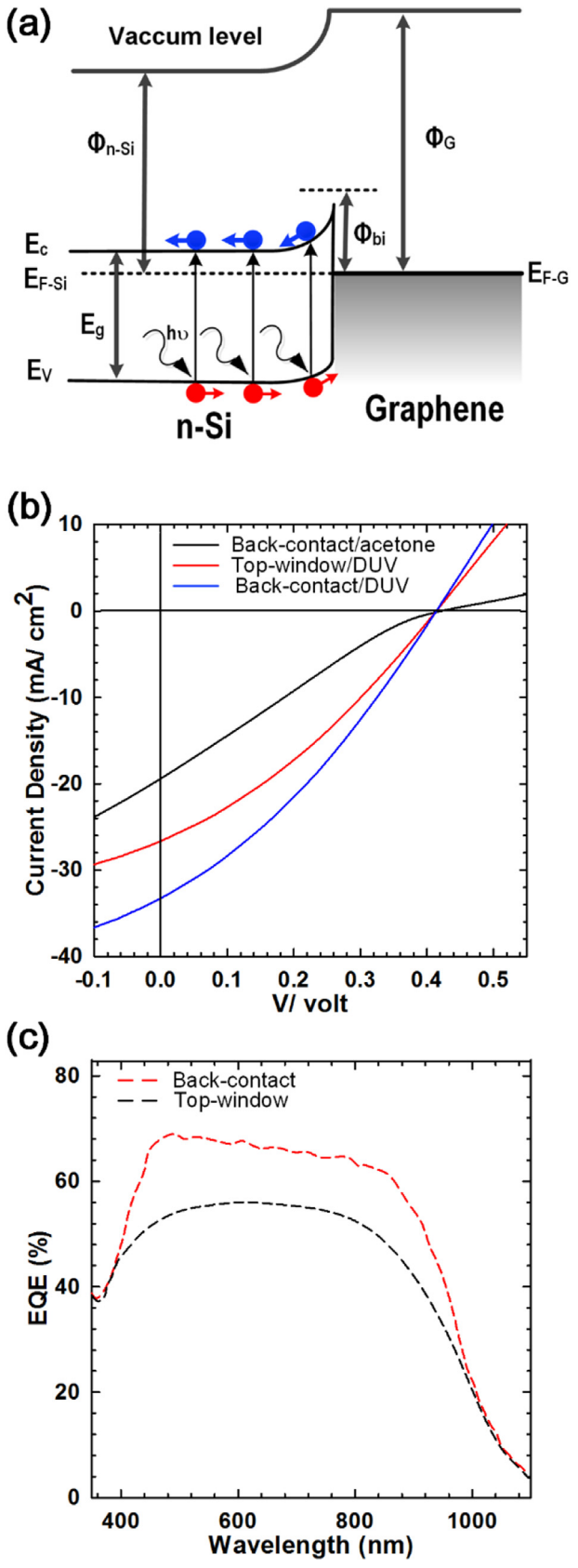

Fig. 2. (a) Schematic energy diagram of device and photoexcited electron transfer. (b) *J-V* characteristics for the graphene/Si Schottky solar cells fabricated with top-window and back-contact structures. (c) External quantum efficiency (EQE) spectra of devices fabricated with both structures. (A colour version of this figure can be viewed online.)

of graphene devices. The influence of annealing in forming gas (argon/hydrogen (9:1)) on the elimination of s-shape is also studied in this work. After transferring PMMA/graphene onto a Si substrate, PMMA layer was removed by acetone. Then, the sample was annealed in forming gas at 300 °C and $6x10^{-7}$ Torr for 2 h. Fig. 4 shows the *J-V* curve (black line) of an annealed device. The J_{SC}, V_{OC}, *FF* and *PCE* of this device were 33.1 mA/cm^2, 0.42 V, 29% and 4%, respectively. It can be observed that the J_{SC}, V_{OC} and *PCE* of this device were improved as a result of reducing the PMMA residue and increasing the doping in graphene [17–20], compared with that of the sample treated with acetone only. However, there is still a s-shape in the *J-V* curve of the annealed device. This means that forming gas could not efficiently eliminate the s-shape in *J-V* curve of graphene/Si Schottky junction solar cells.

XPS data also verify that there was PMMA residue on the annealed graphene for 120 min as shown in Fig. 5b. This states that forming gas (Ar/H_2 (9:1)) treatment would not remove the PMMA residue effectively as also confirmed in reported work [18], compared with DUV treatment between 20 and 60 min. This is a further confirmation that removing the PMMA residue is the key to eliminate the s-shape of graphene/Si Schottky junction solar cells.

Due to the novelty of our structure, texturing process could effectively be involved within the fabrication process to reduce the reflected light from the front surface of Si substrates (see Fig. 6a). Thus, the average diffused reflectance (R) of the textured substrate using process c (see Table S3 and Fig. S6) could be reduced from 39% to 13% within the range of 400–700 nm. Fig. 6b shows the *J-V* characteristics of graphene/n-textured Si before and after applying chemical doping. As shown in this figure (black line), the values of J_{SC}, V_{OC}, *FF* and *PCE* for the graphene/n-textured Si device were 40 mA/cm^2, 0.51 V, 49% and 10%, respectively. This means that the *PCE* was increased by 60% in comparison with that of non-textured substrate devices. To the best of our understanding, the *PCE* of 10% is a new record for graphene/Si solar cells prepared without chemical doping and anti-reflection coating reported to date [2,4,6,32].

After treating graphene sheet with 65% HNO_3 vapor for 60 s, the corresponding values of the photovoltaic parameters were 40.8 mA/cm^2, 0.61 V, 57% and 14.1%, respectively. It is clear that the measured *J-V* curve (red line) of the doped device displayed a noteworthy enhancement in photovoltaic performance compared to that of the non-treated device with HNO_3. The improvement of solar cell performance after the doping process was a result of the enhancements in J_{SC}, V_{OC} and *FF*, unlike reported devices treated with HNO_3 [4,8]. This attributes to the improved electrical conductivity of graphene after reducing the PMMA residue and chemical doping process [23,33]. To study the stability of the chemical doped devices, samples were kept in ambient conditions for 9 days. The measurement of *J-V* curves was repeated during that time. The average results of measured photovoltaic parameters during 9 days are shown in Fig. 7. It can be noticed from these figures and Table S2 that the drop in the performance of treated devices is mainly because of the decrease of V_{OC}. This is because the chemical dopants gradually evaporate during this time [16,34]. It is also clear from Fig. 6b that the *J-V* curve (blue line) of the doped device is still without s-shape after 9 days, and the *PCE* of this device was 11.83%. This means that the device retains 84% of the efficiency after storage. This also indicates that our devices showed more stability than those treated with HNO_3 in the reported work [16]. Thus, removing the PMMA residue on graphene surfaces plays a vital role in the stability of chemical doped graphene/Si Schottky junction solar cells. The doping level of the graphene layer decreases with time due to evaporation and reduces the overall efficiency of the cell.

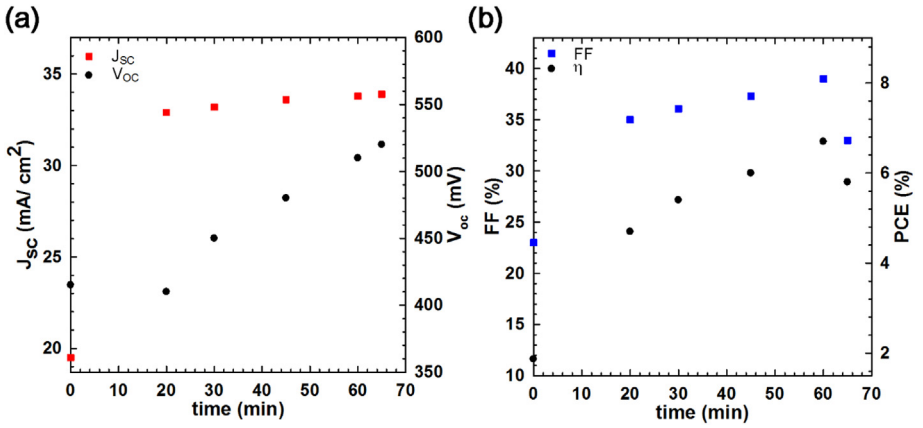

Fig. 3. (a) and (b) Improvements of V_{OC}, J_{SC}, *FF*, and *PCE* of irradiated devices by DUV for different periods. (A colour version of this figure can be viewed online.)

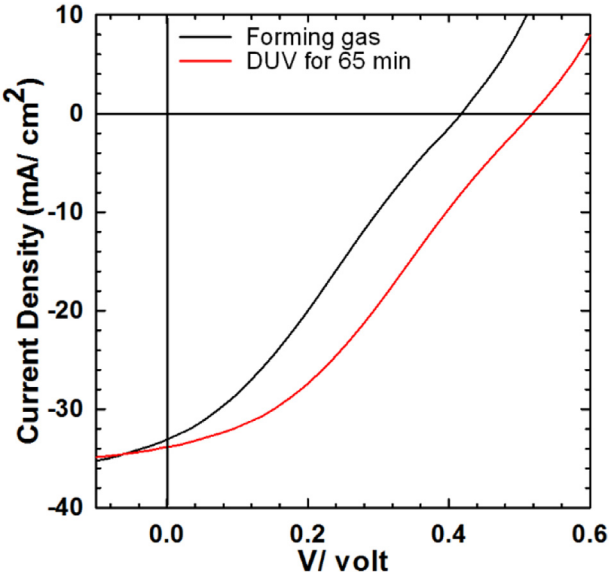

Fig. 4. *J-V* characteristics of graphene/n-Si Schottky junction solar cells treated with forming gas at 300 °C for 120 min and DUV at 180 °C for 65 min. (A colour version of this figure can be viewed online.)

4. Conclusions

We demonstrated the role of a back-contact structure on the graphene/Si Schottky junction solar cell efficiency. With this structure, the short-circuit current density was improved by around 25% compared with that of the device fabricated with the top-window structure. The issue of recombination processes for charge carriers at the graphene/textured Si interface was also prevented by using this structure. Besides, we practically found that PMMA residue is the key to eliminate the s-shaped kink in *J-V* curves of graphene/Si Schottky junction solar cells. This shape was successfully eliminated using the DUV treatment in air for 20 min. Additionally, applying the DUV treatment between 30 and 60 min could further reduce the PMMA residue and enhance p-doping in graphene, leading to a further improvement in the solar cell efficiency. After applying the texturing process and chemical doping, the power conversion efficiency of 14.1% was obtained for graphene/Si Schottky junction solar cell. This device also showed great stability after 9 days storage, and it could retain about 84% of the efficiency. This work presents a feasible way to preparing low-cost and high-performance graphene/Si Schottky junction solar cells.

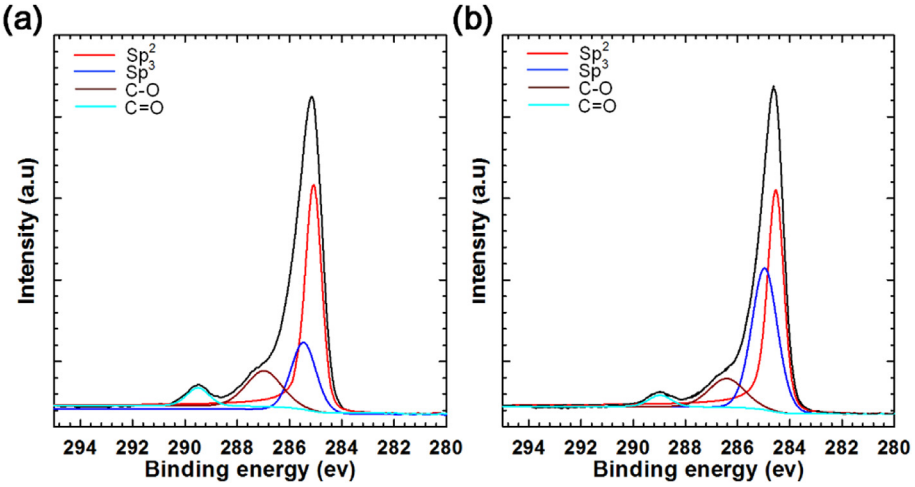

Fig. 5. (a) and (b) XPS results of treated graphene on SiO_2/Si substrates with DUV at 180 °C for 65 min and forming gas at 300 °C for 120 min, respectively, the red peak corresponds to graphene, and the others indicate PMMA residue. (A colour version of this figure can be viewed online.)

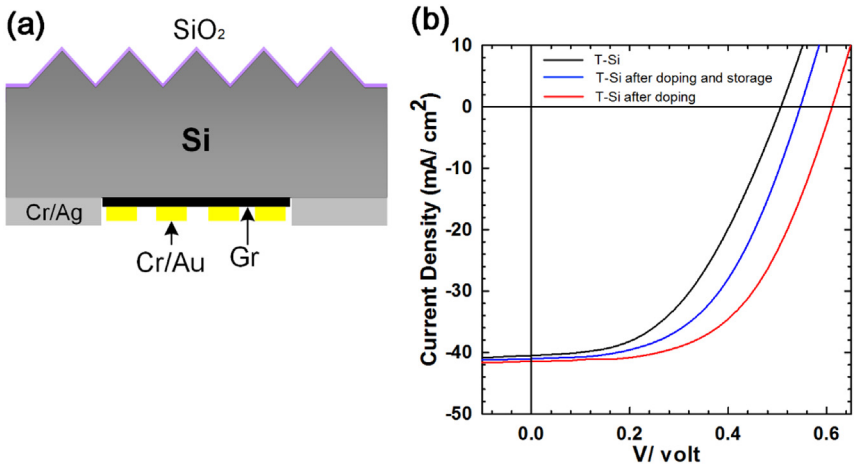

Fig. 6. (a) Schematic of graphene/textured Si Schottky junction solar cell, indicating SiO_2 as the passivation layer. (b) *J-V* characteristics for graphene/textured Si devices before and after doping process. (A colour version of this figure can be viewed online.)

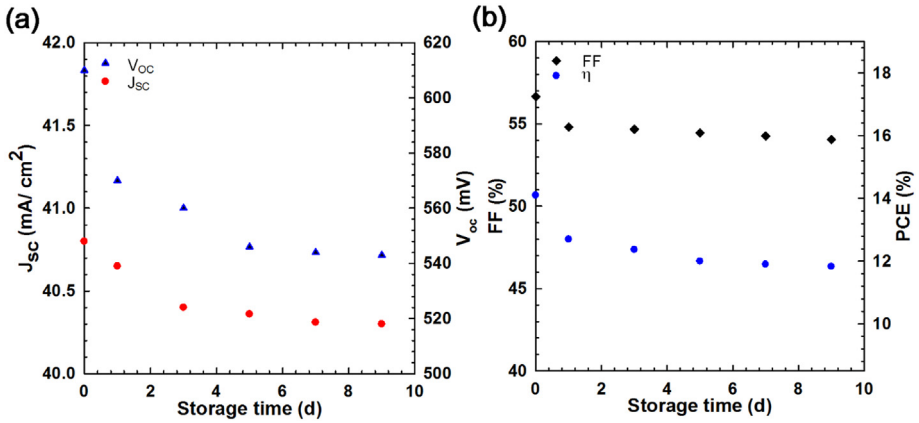

Fig. 7. (a) and (b) Photovoltaic parameters of chemical doped graphene/Si Schottky junction solar cells during 9 days storage in air. (A colour version of this figure can be viewed online.)

Acknowledgment

We acknowledge the financial support by The Higher Committee for Education Development in Iraq under the Grant No. D-11-2969.

Appendix A. Supplementary data

Supplementary data related to this article can be found at https://doi.org/10.1016/j.carbon.2017.12.053.

References

[1] K.S. Novoselov, V. Fal, L. Colombo, P. Gellert, M. Schwab, K. Kim, A roadmap for graphene, Nature 490 (7419) (2012) 192–200.
[2] Y. Wang, C. Chen, X. Fang, Z. Li, H. Qiao, B. Sun, Q. Bao, Top-grid monolayer graphene/Si Schottkey solar cell, J. Solid State Chem. 224 (2015) 102–106.
[3] X. Li, H. Zhu, K. Wang, A. Cao, J. Wei, C. Li, Y. Jia, Z. Li, X. Li, D. Wu, Graphene-on-silicon Schottky junction solar cells, Adv. Mater. 22 (25) (2010) 2743–2748.
[4] Y. Song, X. Li, C. Mackin, X. Zhang, W. Fang, T.s. Palacios, H. Zhu, J. Kong, Role of interfacial oxide in high-efficiency graphene–silicon Schottky barrier solar cells, Nano Lett. 15 (3) (2015) 2104–2110.
[5] Y. Lin, X. Li, D. Xie, T. Feng, Y. Chen, R. Song, H. Tian, T. Ren, M. Zhong, K. Wang, Graphene/semiconductor heterojunction solar cells with modulated antireflection and graphene work function, Energy Environ. Sci. 6 (1) (2013) 108–115.
[6] L. Yang, X. Yu, M. Xu, H. Chen, D. Yang, Interface engineering for efficient and stable chemical-doping-free graphene-on-silicon solar cells by introducing a graphene oxide interlayer, J. Mater. Chem. 2 (40) (2014) 16877–16883.
[7] X. An, F. Liu, S. Kar, Optimizing performance parameters of graphene–silicon and thin transparent graphite–silicon heterojunction solar cells, Carbon 57 (2013) 329–337.
[8] E. Shi, H. Li, L. Yang, L. Zhang, Z. Li, P. Li, Y. Shang, S. Wu, X. Li, J. Wei, Colloidal antireflection coating improves graphene–silicon solar cells, Nano Lett. 13 (4) (2013) 1776–1781.
[9] Y. Shi, K.K. Kim, A. Reina, M. Hofmann, L.-J. Li, J. Kong, Work function engineering of graphene electrode via chemical doping, ACS nano 4 (5) (2010) 2689–2694.
[10] P. Wadhwa, B. Liu, M.A. McCarthy, Z. Wu, A.G. Rinzler, Electronic junction control in a nanotube-semiconductor Schottky junction solar cell, Nano Lett. 10 (12) (2010) 5001–5005.
[11] P. Wadhwa, G. Seol, M.K. Petterson, J. Guo, A.G. Rinzler, Electrolyte-induced inversion layer Schottky junction solar cells, Nano Lett. 11 (6) (2011) 2419–2423.
[12] X. An, F. Liu, Y.J. Jung, S. Kar, Tunable graphene–silicon heterojunctions for ultrasensitive photodetection, Nano Lett. 13 (3) (2013) 909–916.
[13] W. Regan, S. Byrnes, W. Gannett, O. Ergen, O. Vazquez-Mena, F. Wang, A. Zettl, Screening-engineered field-effect solar cells, Nano Lett. 12 (8) (2012) 4300–4304.
[14] X. Li, D. Xie, H. Park, T.H. Zeng, K. Wang, J. Wei, M. Zhong, D. Wu, J. Kong, H. Zhu, Anomalous behaviors of graphene transparent conductors in graphene–silicon heterojunction solar cells, Adv. Eng. Mater. 3 (8) (2013) 1029–1034.
[15] L. Yang, X. Yu, W. Hu, X. Wu, Y. Zhao, D. Yang, An 8.68% efficiency chemically-doped-free graphene–silicon solar cell using silver nanowires network buried contacts, ACS Appl. Mater. Interfaces 7 (7) (2015) 4135–4141.
[16] T. Cui, R. Lv, Z.-H. Huang, S. Chen, Z. Zhang, X. Gan, Y. Jia, X. Li, K. Wang, D. Wu, Enhanced efficiency of graphene/silicon heterojunction solar cells by molecular doping, J. Mater. Chem. 1 (18) (2013) 5736–5740.

[17] Y. Choi, J. Lee, J. Seo, S. Jung, U. Kim, H. Park, The effect of the graphene integration process on the performance of graphene-based Schottky junction solar cells, J. Mater. Chem. 5 (35) (2017) 18716–18724.
[18] W. Choi, Y.-S. Seo, J.-Y. Park, K. Kim, J. Jung, N. Lee, Y. Seo, S. Hong, Effect of annealing in Ar/H 2 environment on chemical vapor deposition-grown graphene transferred with poly (methyl methacrylate), IEEE Trans. Nanotechnol. 14 (1) (2015) 70–74.
[19] Z.H. Ni, H.M. Wang, Y. Ma, J. Kasim, Y.H. Wu, Z.X. Shen, Tunable stress and controlled thickness modification in graphene by annealing, ACS nano 2 (5) (2008) 1033–1039.
[20] Y.-C. Lin, C.-C. Lu, C.-H. Yeh, C. Jin, K. Suenaga, P.-W. Chiu, Graphene annealing: how clean can it be? Nano Lett. 12 (1) (2011) 414–419.
[21] A.G. Aberle, Surface passivation of crystalline silicon solar cells: a review, Prog. Photovoltaics Res. Appl. 8 (5) (2000) 473–487.
[22] B.-S. Wu, Y.-C. Lai, Y.-H. Cheng, S.-C. Yu, P. Yu, G.-C. Chi, Hybrid multi-layer graphene/Si Schottky junction solar cells, in: Photovoltaic Specialists Conference (PVSC), 2013 IEEE 39th, IEEE, 2013, pp. 2486–2489.
[23] A. Suhail, K. Islam, B. Li, D. Jenkins, G. Pan, Reduction of polymer residue on wet–transferred CVD graphene surface by deep UV exposure, Appl. Phys. Lett. 110 (18) (2017), 183103.
[24] Y. Xu, C. Cheng, S. Du, J. Yang, B. Yu, J. Luo, W. Yin, E. Li, S. Dong, P. Ye, Contacts between two-and three-dimensional materials: ohmic, schottky, and p–n heterojunctions, ACS nano 10 (5) (2016) 4895–4919.
[25] X. Miao, S. Tongay, M.K. Petterson, K. Berke, A.G. Rinzler, B.R. Appleton, A.F. Hebard, High efficiency graphene solar cells by chemical doping, Nano Lett. 12 (6) (2012) 2745–2750.
[26] S. Riazimehr, S. Kataria, R. Bornemann, P. Haring-Bolivar, F.J.G. Ruiz, O. Engström, A. Godoy, M.C. Lemme, High photocurrent in gated graphene-silicon hybrid photodiodes, ACS Photonics 4 (6) (2017) 1506–1514.
[27] C.J. An, S.J. Kim, H.O. Choi, D.W. Kim, S.W. Jang, M.L. Jin, J.-M. Park, J.K. Choi, H.-T. Jung, Ultraclean transfer of CVD-grown graphene and its application to flexible organic photovoltaic cells, J. Mater. Chem. 2 (48) (2014) 20474–20480.
[28] J.W. Suk, W.H. Lee, J. Lee, H. Chou, R.D. Piner, Y. Hao, D. Akinwande, R.S. Ruoff, Enhancement of the electrical properties of graphene grown by chemical vapor deposition via controlling the effects of polymer residue, Nano Lett. 13 (4) (2013) 1462–1467.
[29] J. Nelson, The Physics of Solar Cells, World Scientific Publishing Co Inc, 2003.
[30] M. Iqbal, M. Iqbal, M. Khan, J. Eom, Ultraviolet-light-driven doping modulation in chemical vapor deposition grown graphene, Phys. Chem. Chem. Phys. 17 (32) (2015) 20551–20556.
[31] K.S. Kim, Y. Zhao, H. Jang, S.Y. Lee, J.M. Kim, K.S. Kim, J.-H. Ahn, P. Kim, J.-Y. Choi, B.H. Hong, Large-scale pattern growth of graphene films for stretchable transparent electrodes, Nature 457 (7230) (2009) 706–710.
[32] S.H. Kim, J.H. Lee, J.-S. Park, M.-S. Hwang, H.-G. Park, K.J. Choi, W.I. Park, Performance optimization in gate-tunable Schottky junction solar cells with a light transparent and electric-field permeable graphene mesh on n-Si, J. Mater. Chem. C 5 (12) (2017) 3183–3187.
[33] S. Tongay, K. Berke, M. Lemaitre, Z. Nasrollahi, D. Tanner, A. Hebard, B. Appleton, Stable hole doping of graphene for low electrical resistance and high optical transparency, Nanotechnology 22 (42) (2011), 425701.
[34] E. Singh, H.S. Nalwa, Stability of graphene-based heterojunction solar cells, RSC Adv. 5 (90) (2015) 73575–73600.